Conceptual design and numerical simulation of a correlation diagnostic for measurement of magnetic fluctuations in plasmas

C. E. Thomas Jr., G. R. Hanson, R. F. Gandy, D. B. Batchelor, and R. C. Goldfinger

Citation: Review of Scientific Instruments **59**, 1990 (1988); doi: 10.1063/1.1140064
View online: http://dx.doi.org/10.1063/1.1140064
View Table of Contents: http://scitation.aip.org/content/aip/journal/rsi/59/9?ver=pdfcov
Published by the AIP Publishing

Conceptual design and numerical simulation of a correlation diagnostic for measurement of magnetic fluctuations in plasmas[a)]

C. E. Thomas Jr. and G. R. Hanson

Nuclear Engineering Program, Georgia Institute of Technology, Atlanta, Georgia 30332

R. F. Gandy

Department of Physics, Auburn University, Auburn, Alabama 36849

D. B. Batchelor and R. C. Goldfinger

Fusion Energy Division, Oak Ridge National Laboratory, Oak Ridge, Tennessee 37831

(Received 15 March 1988; accepted for publication 20 April 1988)

It has been previously suggested that crossed-sightline correlation of electron cylotron emission might be used to measure magnetic fluctuations in high-temperature plasmas. Reported here are the results of a continuing project to determine under what conditions (if any) this measurement will be feasible. An initial conceptual design for the device hardware has been completed. Large portions of the numerical simulation are working, including ray-tracing and emission/absorption packages. An initial discussion of data analysis for the experimental data is presented, and an analysis of the uncertainty in the line center (magnetic field) measurement in terms of the experimental uncertainties is given.

INTRODUCTION

Electron energy transport in fusion experiments steadfastly refuses to be classical or neoclassical.[1,2] It is widely suspected that local fluctuations could be the cause of the anomalous transport, and the state of theory and experiment in this area has been recently reviewed.[3] One possible candidate as the cause of this anomalous transport is local fluctuation of the magnetic field.[4–7]

It has been suggested that crossed-sightline correlation of electron cyclotron emission (ECE) might be used to experimentally measure magnetic fluctuations in high-temperature plasmas.[8] The idea is very briefly reviewed here (for more depth see Ref. 8). Suppose that there are two ECE antennas with crossed sightlines into the plasma (see Fig. 1), and let $I_1(\omega_i,t)$ be the signal out of the microwave detector in some passband $\delta\omega_i$ about frequency ω_i at time t, and similarly for $I_2(\omega_i,t)$. Then let $\langle\ \rangle$ be defined as the equal-time correlation function operator [see Eq. (13)]. Then

$$\langle I_1(\omega_i,t)I_2(\omega_i,t)\rangle = \left\langle \int ds_1 \int ds_2\, i_1(\omega,s_1,t) i_2(\omega,s_2,t) \right\rangle, \tag{1}$$

where it is assumed that I_1 and I_2 are high-pass filtered and i_1 and i_2 are the local values of the fluctuating part of the emission at positions s_1 and s_2 [the fluctuating part of dP_{ant} in Eq. (10)]. By definition, in regions of a turbulent plasma that are separated by more than a correlation length l_c, the time correlation (cross-correlation) function rapidly goes to zero, in which case Eq. (1) can be written as

$$\langle I_1(\omega_i,t)I_2(\omega_i,t)\rangle = \int_{r_x-l_c}^{r_x+l_c} ds_1 \int_{r_x-l_c}^{r_x+l_c} ds_2 \langle i_1(\omega,s_1,t) i_2(\omega,s_2,t)\rangle, \tag{2}$$

where r_x is the spatial crossing point of the two sightlines, and the time operator has been passed through the two spatial integrals.

It can be seen from the above equation that as the correlation length becomes small, the cross correlation of I_1 and I_2 comes only from the crossing volume of the two Gaussian beams forming the sightlines (we assume Gaussian antenna patterns as discussed further below). If the magnetic fluctuations of interest have a wavelength longer than the length of the sightline crossing volume, and their frequency is less than $1/T$, where T is the effective time for the cross correlation, then the frequency of the line center of the cross-correlation function of I_1 and I_2 will vary linearly in time with the magnitude of the magnetic field fluctuation. This is the idea at the heart of our interest in building an ECE diagnostic to measure magnetic fluctuations.

A conceptual design, numerical analysis, and data analysis for such a diagnostic are discussed below.

I. CONCEPTUAL DESIGN

A. Design target

In order to make the design concrete, and aimed at an actual experimental fusion device (on which we hope to mount the system), the TEXT tokamak (Fusion Research Center, University of Texas, Austin, Texas) is chosen as the target for the design. The nominal magnetic field is chosen as $B_0 = 2$ T on-axis, and the nominal central plasma density as $n_e = 5\times10^{19}$ m^{-3}, the plasma current as $I_p = 150$ kA, and the density, temperature, and current profiles as $Q(r) = Q_0[1-(r/a)^n]^m + Q_a$, where Q is the quantity of interest, Q_0 is the central value, r is the radius in the plasma, a is the plasma minor radius, n is normally 2, m is normally 1 or 2, and Q_a is the edge value. All of these are typical parameters, but the conceptual design can be scaled as necessary. The TEXT tokamak has a minor radius $a = 30$ cm and a

 0034-6748/88/091990-08$01.30

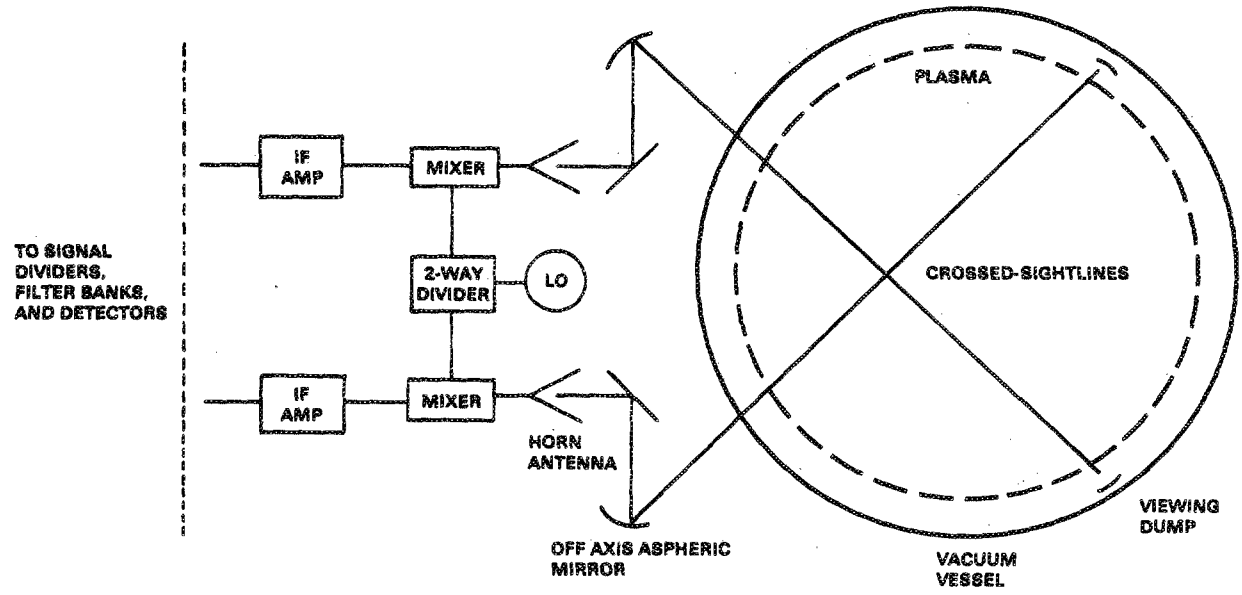

FIG. 1. Conceptual schematic of the antenna system, viewing sightlines and dumps, and mixer, LO, and IF amplifier for the crossed-sightline system.

major radius $R_0 = 1$ m. The third-harmonic ECE frequency at $r/a = 0.5$ on the outboard major radius of the device is chosen as the nominal ECE frequency at the sightline crossing, which is chosen as above ($r/a = 0.5$, $R > R_0$, on the horizontal centerline; see Fig. 1).

B. Viewing sightlines

Choosing a viewing sightline involves tradeoffs between a number of constraints. The first choice is whether to view perpendicular or parallel to the magnetic field or somewhere in between. The answer to this question is dictated by linewidths. As the viewing angle becomes more parallel to the field, the linewidth of the ECE is dominated by the Doppler shift and becomes excessively large for the intended purpose of measuring the magnetic field. Trying to measure a frequency shift of 1×10^{-4} of a line whose width is 5×10^{-2} is perhaps too difficult. There are enough problems when the natural linewidth is only 5×10^{-3} of the line center. This will be discussed further under the data analysis section. It appears that the viewing sightlines must be perpendicular to the magnetic field.

The next choice for the viewing sightlines is whether to place them horizontally in the poloidal plane, vertically in the poloidal plane, or at some angle in between. We believe that the correct choice is a symmetric combination. There are several requirements to be considered here. The first is minimizing the spatial linewidth of the signal. The minimum spatial linewidth (assuming the emitting volume for correlation is approximately the volume of the crossed antenna patterns), occurs when the antenna patterns intersect at a 90° angle. However, placing one sightline on the horizontal midplane and the other sightline vertically, an initially attractive thought, causes trouble when signal-to-noise ratios are considered. For short correlation lengths, all of the signal at a frequency ω that did not originate within a correlation length of the crossing volume is noise. As will be discussed in the data analysis section, this leads to a smaller cross-correlation coefficient, and ultimately to increased uncertainty in the line center and, therefore, the magnetic field at the crossing point. For vertical sightlines the emission frequency is constant along the whole sightline, since verticality defines a surface of constant mod B in a tokamak. The signal-to-noise ratio will be unacceptable for a vertical sightline. The optimum choice would be two horizontal sightlines crossing at 90°, but as discussed in the paragraph above, this leads to an unacceptable linewidth. The apparent optimum is to choose symmetric sightlines in the poloidal plane which cross at as close to 90° as is consistent with the available port geometry into the tokamak. In addition, the viewing sightlines must be chosen to facilitate placing viewing dumps in the tokamak for each sightline. This is crucial in maximizing the signal-to-noise ratio.

C. Antennas

The optimum antenna would have an antenna pattern with an angular spread that is a function of the correlation length and spatial linewidth at the beam crossing point (the antenna would be matched to the desired volume). Here the spatial linewidth is the spatial distance which must be moved to cause a change in the rest mass cyclotron frequency equal to the frequency linewidth at a fixed spatial point due to relativistic broadening. In the end, the antenna beamwidth will be chosen to minimize the cross-correlated linewidth in frequency space, and to maximize the correlation coefficient (minimize the noise-to-signal ratio). If the fluctuation correlation length and spatial linewidth are quite different, then there will be a tradeoff in the optimum antenna design, which will depend on the central wavelength of the fluctuations being investigated. If the correlation length and spatial linewidth are about the same, then the antenna pattern should be chosen to match the spatial linewidth. This is discussed further below. A convenient antenna design for try-

ing to achieve this is the Gaussian antenna pattern.[9–11] This pattern offers peaking of the antenna gain at the beam center with rapid falloff at the edge, and allows diffraction-limited performance.[12] It also offers considerable advantages when trying to make analytic approximations to the signal and line shape.

It is expected that the antenna system will consist of an off-axis elliptical reflector, combined with a corrugated horn. This combination will allow spatial scanning by translating and rotating the reflectors, without movement of the microwave system. In addition, the reflector system can be easily aligned with a He–Ne laser. If the crossed-sightline antennas are mounted on a rigid structure which can be pulled back from the tokamak, then alignment can be performed without breaking the tokamak vacuum.

D. Ports and viewing dumps

The ports must be designed so as to avoid Fabry–Pérot resonances. This will require ensuring that the window dimension is not close to a half-integer number of wavelengths, and possibly wedging the faces of the windows slightly. In order to preserve the diffraction-limited nature of the proposed Gaussian beam optical design, the ports should be flat to $\lambda/10$, which is not difficult at these wavelengths. The viewing dumps should be made from a material that is highly absorptive at the frequency of interest, and it is expected that a grooved Macor design based on the work of Kato and Hutchinson[13,14] will be used. The viewing dumps are a crucial part of the diagnostic design. The design goal will be to make them 99% absorptive, which will reduce the expected reflected (and uncorrelated) signal to less than 10% of the sightline signal at any frequency ω on the sightline (this assumes the vacuum vessel walls are 90% reflective).

E. Microwave system design

A number of different designs have been used for ECE microwave systems.[15–18] These include Michelson systems, grating polychromators, filter bank systems, heterodyne systems, and scanning heterodyne systems. The present conceptual design for the crossed-sightline system (see Figs. 1 and 2) is a heterodyne system with filter banks, based on the ATF design.[11]

The signals from the ridged horns discussed above will be fed into two mixers, sharing the same local oscillator (this should help eliminate noise when the cross-correlation coefficient is calculated and will eliminate any frequency offsets between the two sightlines). The expected signal frequency halfway out in the tokamak is $f \approx 146$ GHz (for a 2-T on-axis field). Thus for a 10-GHz IF (intermediate frequency), the local oscillator (LO) frequency should be chosen to be

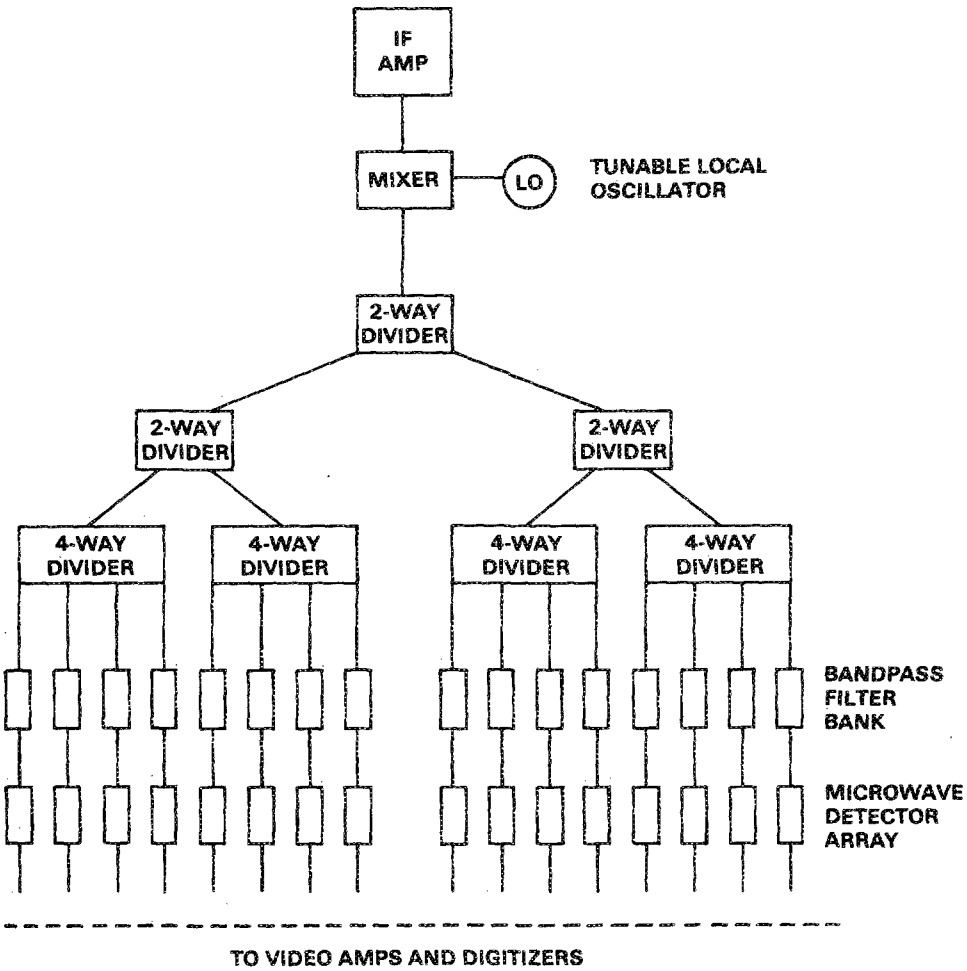

FIG. 2. Conceptual schematic of the balance of the microwave electronics for the crossed-sightline ECE system (see Fig. 1 for the front end).

136 GHz. The IF amplifier will be chosen to have approximately a 13-GHz bandwidth from 3.5 to 16.5 GHz. Following the IF amplifier will be another mixer and shared tunable LO, with a frequency range from about 2 to 12 GHz. The tunable LO will provide tuning of the central passband frequency which is fed into the filter bank over about a 10-GHz (or $\approx$6-cm) range (with the central filter frequency at 3 GHz) to allow for varying the magnetic fields or sweeping the sightline crossing position. Further spatial tuning can be achieved by varying the tokamak magnetic field and the sightline crossing position simultaneously. Each individual filter will have a 150-MHz passband, and the band centers will be chosen about 150 MHz apart, so that the total coverage of the 20 channels in each filter bank will be 3 GHz, centered around a 3-GHz IF frequency (note that the number of channels indicated in Fig. 2 is purely schematic; the actual number of channels will probably be determined by cost). The large difference in the IF is chosen so that the LO signal will not contaminate the plasma signals. Note that the high-frequency LO (136 GHz here) must be frequency stable to 1 part in 10^5 over a time period of about 1 s, to prevent contamination of the data. This is relatively easy to achieve.

Following each microwave filter will be a microwave detector. The detector signals will be buffered and then either fed directly into analog correlators to produce (where we designate the two microwave signals from the plasma as 1 and 2) C_{12}, C_{11}, and C_{22} and then digitized, or high-pass filtered (at something like 100 Hz) and digitized directly. The symbols C_{ij} stand for the cross-correlation (12) and autocorrelation (11,22) functions. The most attractive alternative is to digitize the buffered detector signals directly, at about 1 MHz. However, the cost of the CAMAC modules and the amount of data produced (about 4 Mbytes for a 100-ms shot) may make it necessary to use the analog correlators, which will reduce the data rate to about 100 kHz or less, since it is not necessary to have the fast-time data if the signals have already been correlated. The problem with using the hardware correlation is that it cannot be changed after the shot. If the data are digitized directly, then the correlation time can be experimented with on the computer to find the optimum correlation period, or to produce different kinds of data (for instance, the data could be digitally high-pass filtered to look at only fluctuations above 100 kHz or vice versa).

II. NUMERICAL SIMULATION

A. Local emission and absorption

The numerical modeling of power emission is much like that of Celata and Boyd,[19] except that we use the RAYS[20] code to model the tokamak geometry and actually trace the ray path through the tokamak. The numerical modeling here also allows for the possibility of off-perpendicular sightlines. The local emitted and absorbed power calculation is essentially identical to that of Celata and Boyd. We review it briefly for convenience only. The RAYS code will be discussed further below.

The intensity of the cyclotron radiation emitted from a plasma is obtained by integrating the radiation from a single electron over the distribution function in velocity space. This is formally given by

$$j_{\omega,s} = \int d^3v \left[P(s,\omega_b,\theta,\mathbf{v}) \times \delta\left(\omega - \frac{s\omega_b (1 - v^2/c^2)^{1/2}}{1 - (v_\parallel/c)\cos\theta} \right) f(\mathbf{r},\mathbf{v},t) \right], \quad (3)$$

where $j_{\omega,s}$ is the power radiated per unit volume, solid angle, and frequency interval in the sth harmonic, ω_b is the fundamental electron cyclotron frequency calculated with the electron rest mass, θ is the angle between the magnetic field and the angle of observation, $f(\mathbf{r},\mathbf{v},t)$ is the electron distribution function, and $P(s,\omega_b,\theta,\mathbf{v})$is the power radiated by a single electron per unit solid angle in the sth harmonic. The dirac delta function $\delta(\ )$ defines the constant-frequency surface over which the integral is performed.[21,22]

The power emitted by a single electron per unit solid angle is a difficult function of velocity, magnetic field, frequency, and angle with respect to the magnetic field. This calculation is not reproduced here (see Refs. 21 or 22). For perpendicular viewing and Maxwellian distributions, Eq. (3) can be integrated exactly[19]; otherwise the integral must be performed numerically.

To solve the integral in Eq. (3) numerically, the integration is performed in cylindrical velocity coordinates. We have used the nonrelativistic Maxwellian distribution function to simplify the calculations. This simplification has a negligible effect on the power emission calculations as the plasmas of interest in our studies are in the 1–5-keV range. However, any distribution function, such as the relativistic Maxwellian, can be easily substituted into the numerical calculations. The two variables of integration are the perpendicular velocity with integration limits of zero to an arbitrary number of e foldings (e^n, $n = 1, 2, \ldots$)of the distribution function, and the parallel velocity with limits of minus to plus the same arbitrary number of e foldings (typically four or five). For the case where the emission from a volume element is being studied, the maximum and minimum emission frequency from the volume must be determined. The delta function can be used to determine the region in velocity space within a spatial volume which contributes radiation in the desired frequency band. The maximum and minimum frequencies are a function of the change in the magnetic field strength over the spatial volume and the Doppler and relativistic frequency shift and broadening.[19,22]

For thermal plasmas, Kirchhoff's law can be used to find the local absorption,[23] since the emission is calculated above. The absorption coefficient can be found from

$$j_\omega / n_r^2 \alpha_\omega = B_0(\omega,t). \quad (4)$$

The function $B_0(\omega,t)$ is the familiar vacuum blackbody intensity given by the Rayleigh–Jeans law in the classical limit ($\hbar\omega/kT \ll 1$),

$$B_0(\omega,t) = (\omega^2/8\pi^3c^2)kT, \quad (5)$$

and has units of W/(m^2 sr Hz). Also, T is the plasma electron temperature, k is Boltzmann's constant, t is time, j_ω is the emission coefficient $j_{\omega,s}$ summed over harmonics s, with units of W/(m^3 sr Hz), α_ω is the absorption coefficient with

units of inverse meters, and n_r is the ray refractive index and is easily obtained from the RAYS code.

B. Ray tracing

At the heart of the numerical simulation is the need to trace electromagnetic waves through the plasma. The RAYS code is used to perform this ray tracing. RAYS was developed at ORNL to study the propagation and absorption of electromagnetic waves in an arbitrary, three-dimensional, magnetized plasma configuration.[20] The ray tracing is carried out by integrating the Hamiltonian form of the geometrical optics equations using the two-component, cold plasma dispersion relations. The code is written in modular form. The subroutines specify the plasma equilibrium magnetic field and density and the independence of the wave dispersion relations. The RAYS code provides an excellent base for numerical simulation of the crossed-sightline correlation of cyclotron emission into Gaussian antennas. Although the code is designed to trace a ray from a launching point, i.e., antenna, through the plasma until it is either absorbed, cut off, or leaves the plasma, we are modeling emission from the plasma into the antenna. It is assumed that the path of the central ray from the Gaussian antenna includes all the points emitting cyclotron radiation incident on the antenna. That is, we take the density, temperature, and magnetic field as constant perpendicular to the ray path. This assumption is not basic to the numerical modeling, but is not inconsistent with our requirements, and will be used until finer-scale information is required. In the emitting volume of interest (approximately at the beam waist and crossing point of the two Gaussian beams), the assumption is reasonable since the beam diameter will be small (of the order of a centimeter). The real approximation here is that the fluctuation wavelengths are larger than the beam diameter. For fluctuation wavelengths shorter than the beam diameter, it can be shown[24] that the fluctuation power integral rapidly goes to zero (though not the average power); therefore, we are not really interested in modeling fluctuations that violate our assumption.

A version of the RAYS code that uses a simple axisymmetric, circular cross-section tokamak model is employed. The starting position and direction of the ray are read in from a data file (specified by the user). The ray tracing is then controlled by a set of nested do-loops. Minor changes have been made to the code to allow for the crossed-beam configuration and emission calculations. The modifications allow for specifying two ray launch locations on the edge of the plasma and a point within the plasma where the rays will intersect. See Fig. 3 for a typical sample of ray paths at the third harmonic of the crossing point for two rays in TEXT. The central magnetic field was 2 T, and the central density $n_e = 6\times10^{19}\ \mathrm{m}^{-3}$.

In the millimeter wavelengths associated with the cyclotron radiation, it has proven advantageous to use Gaussian beam optics in treating propagating waves.[11] A Gaussian beam is a propagating wave front with a two-dimensional Gaussian-shaped field profile. An excellent treatment of this quasioptical approach to wave-front propagation is given by

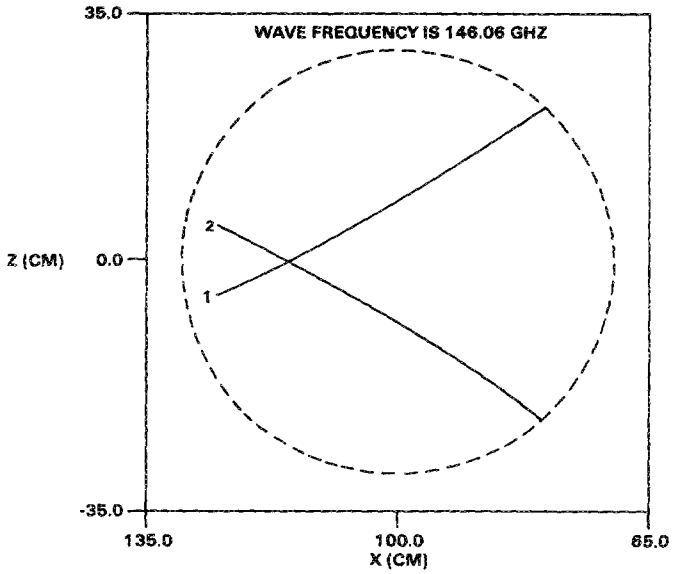

FIG. 3. X–Z plot of ray paths. Output of RAYS code showing ray path through a typical TEXT plasma at 146 GHz. The numbers 1 and 2 indicate paths.

Kogelnik and Li.[10] Physically, a Gaussian beam provides the advantages of easy modeling, a narrow beamlike diffraction-limited antenna pattern, and a small beam diameter at the focal point or waist. The actual Gaussian beam, i.e., the proper phase front curvature, can be produced with either a lens or antenna.[9,11]

In our numerical modeling, we have assumed two Gaussian beams with radii described by[10]

$$w(z) = w_0[1 + (\lambda z/\pi w_0^2)^2]^{1/2}, \tag{6}$$

where $w(z)$ is the beam radius (e^{-1} radius) at a distance z measured from the beam waist, and w_0 is the beam radius at the waist. The volume of intersection or crossing volume of the two beams has been determined to be

$$V = (32w_0^3/9)\csc\Psi, \tag{7}$$

where it has been assumed that the beams are intersecting at their minimum radii or waists and that the change in beam diameter is negligible over the length of intersection of the beams, and Ψ is the angle between the intersecting beams.

C. Fluctuation modeling

Fluctuations in density, temperature, and magnetic field will be numerically modeled. The fluctuations will be assumed to be time harmonic (i.e., not growing or decaying in time) and to have some width Δk_c in wave-vector space, and possibly a spatial variation of their amplitude. The density fluctuations, for example, will be modeled as

$$n(\mathbf{r},t) = n_0(\mathbf{r}) + \tilde{n}(\mathbf{r},t), \tag{8}$$

where $n_0(\mathbf{r})$ is the steady-state portion of $n(\mathbf{r},t)$, and $\tilde{n}(\mathbf{r},t)$ is the fluctuating portion. It is assumed that the average of any of the quantities n_e, T_e, and B is not varying with time for time scales faster than 1×10^{-3} s, usually a very good assumption for tokamaks. Then $\tilde{n}(\mathbf{r},t)$ will be modeled as

$$\tilde{n}(\mathbf{r},t)=\tilde{n}\left(\frac{\int_{r-l_c}^{r+l_c}\exp(i\mathbf{k}_2\cdot\mathbf{r}_2)\exp[-(\mathbf{r}-\mathbf{r}_2)^2/l_c^2]\,d\mathbf{r}_2}{\int_{r-l_c}^{r+l_c}\exp[-(\mathbf{r}-\mathbf{r}_2)^2/l_c^2]\,d\mathbf{r}_2}\right)\times\exp(-i\omega t), \tag{9}$$

where $\tilde{n}$ is a constant. Note that this form for $\tilde{n}(\mathbf{r},t)$ will have a correlation length with itself of l_c, and that wave vectors $\mathbf{k}_2$ are chosen at each position $\mathbf{r}_2$ using a Monte Carlo technique with a Gaussian distribution function $f(\mathbf{k}_2)\propto\exp[-(\mathbf{k}_2-\mathbf{k}_0)^2/(\Delta k_c)^2]$. Once the value of $\mathbf{k}_2$ is chosen for any particular position, that value of $\mathbf{k}_2$ must be remembered until $\mathbf{r}$ is no longer within distance l_c of the position. For stepping in time, a particular value of $\mathbf{k}_2$ will propagate in space and must be remembered until it is no longer within l_c of the correlation volume. This method of choosing $\tilde{n}(\mathbf{r},t)$ ensures that it becomes uncorrelated with itself for distances longer than l_c but is continuous in space and time (although its first derivative will not be continuous).

Similar methods will be used for numerically modeling fluctuations in T_e and B. This part of the numerical simulation has not been implemented at the date of this writing.

D. Integration along sightline

The modular aspect of the RAYS code has been built on by adding in a subroutine to calculate the emitted power density of the cyclotron radiation at an arbitrary point in the plasma. The method used to obtain the emitted power was described earlier. Initial calculations are performed to model the intersection of the two beams to obtain the crossing volume and the frequency band across the volume. The frequency band of the crossing volume determines, as discussed earlier, the volume in velocity space from which the cyclotron radiation of interest is emitted at each point along the ray path. As the RAYS code increments the ray path through the plasma, the emitted power density in the frequency band of the crossing volume is calculated. The power is obtained by multiplying the power density by the emission volume and the frequency step size (typically emission might be calculated in 10-MHz increments). The emission volume is approximated as being a cylinder of radius given by Eq. (6) and length equal to the incremental integration length along the ray path.

The expression for the power emitted into the antenna from a differential length ds along the central ray path, over a differential frequency width $d\omega$, is

$$dP_{\text{ant}}=\int(j_\omega\,d\omega\,ds)(2\pi\rho\,d\rho)\times\left[\exp\left(-\int_s^{s_0}\alpha_\omega\,ds\right)\right]\times\left(\frac{\exp[-\rho^2/w^2(z)]}{\pi w^2(z)}\frac{\lambda^2}{4\pi}\right), \tag{10}$$

where the first term in parenthesis is the local power emission per m^2 sr, the second term in parenthesis is the differential cross-sectional area perpendicular to the ray path, the term in large brackets is the attenuation from the present point on the ray, s, to the antenna position s_0, and the last term, in large parenthesis, is the effective solid angle of a Gaussian beam antenna from radius ρ perpendicular to s, with $w(z)$ the beam radius at position s on the ray. The effective solid angle can be calculated using the definition of the effective antenna area[22] $S(\Theta,\phi)$, and $d\Omega=S(\Theta,\phi)/r^2$. Here λ is the wavelength of the radiation at frequency ω. The outermost integral is the integral over the area perpendicular to the ray path (from $\rho=0$ to $\rho=\infty$), and the integral in the large brackets is just the integral of the attenuation coefficient from s to the antenna. It is assumed that $ds\ll\alpha_\omega^{-1}$.

If $w(z)$ is small compared to the density, temperature, and magnetic field scale lengths and the fluctuation wavelength of interest, then the outer integral in Eq. (10) can be evaluated directly to give

$$dP_{\text{ant}}=\left(\frac{\lambda^2}{4\pi}\right)(j_\omega)\left[\exp\left(-\int_s^{s_0}\alpha_\omega\,ds\right)\right](d\omega\,ds). \tag{11}$$

This quantity is calculated for every ds along the ray path where emission occurs within $d\omega$ of frequency ω, and then a simple but highly precise Simpson's rule integration routine is used to find the total integral of the power received at the antenna, within $d\omega$ of frequency ω, originating along the antenna pattern. Note that since the viewing dump is assumed to be 99% effective, reflected power is ignored for the moment, though it will be considered as a source of noise at the 10% level.

The discussion above implicitly assumes that the electron motions are uncorrelated. A sufficient condition for this to be true is that the electron thermal energy density (random energy) be large compared to the fluctuation energy density [$(kT_e)\gg E_f$]. This is unnecessarily restrictive, however. Since the electron velocity phases will be random with respect to one another, the emitted radiation near the cyclotron harmonic, $s\omega_b$, will be incoherent with respect to the fluctuations if the fluctuation frequency is much less than the cyclotron frequency ($\omega_f\ll\omega_b$). For strong fluctuations near the cyclotron frequency, it would be necessary to perform a different analysis.

E. Simulation of microwave and DAQ systems

Let the signal from the first antenna be denoted $I_1(\omega,t)$ and the signal from the second antenna be $I_2(\omega,t)$. The microwave system essentially rectifies and averages these power signals (converting power to current or voltage) for frequencies less than some τ^{-1} within certain passbands of frequency, $\delta\omega_i$. That is, the output of each microwave filter/detector combination will be a voltage (or current, they differ by the impedance) signal $\hat{I}_1(\delta\omega_i)$, where the caret indicates that the signal has been rectified and time averaged over some interval τ.

The other thing that the microwave and data-acquisition (DAQ) systems do is add noise to the signal. The signal leaving the crystal detector will have an intrinsic noise level specified by[23,25]

$$\langle(\delta\hat{I}_1)^2\rangle^{1/2}/\langle\hat{I}_1\rangle=(1/\delta f_i\tau)^{1/2}, \tag{12}$$

where $\delta f_i=\delta\omega_i/2\pi$. There is more than one way to interpret the cause of this noise, but one possibly intuitive approach is to consider it as the noise due to the underlying process of photons arriving at the detector. The microwave system also adds noise which can generally be expressed in the same

fashion—some average square signal and an equivalent fluctuation level are added by the microwave system.

The addition of the noise signal to the useful signal will be again simulated with a Monte Carlo technique (just as for the fluctuation simulation, discussed above), but the underlying distribution will be assumed to be Poisson, rather than Gaussian. As before, the noise signal itself will be continuous in time and coherent with a coherence time $\approx\tau$, but its derivative will not be continuous. Noise levels typical of the microwave system components will be added in, but it is expected that the natural-signal noise level will dominate any other sources (except for very long τ).

III. DATA ANALYSIS

A. Overview

The output from the numerical simulation routines will be a rather large file which simulates the buffered output from the crystal detectors. It will, therefore, consist of records $\hat{I}_1(\delta\omega_i,t)$ and $\hat{I}_2(\delta\omega_i,t)$ of voltage versus time (at discrete time intervals, one per microsecond for the simulation), of the averaged cyclotron power (averaged over time τ) plus system noise in each microwave passband $\delta\omega_i$. The task at hand is to attempt to convert these signals (or possibly find that they cannot be converted) to measurements of the magnetic field fluctuation. The plan for doing this is to calculate the equal-time cross-correlation and correlation functions C_{12i}, C_{11i}, and C_{22i}, and from them calculate the equal-time correlation coefficient ρ_{12i}. Here the i subscript indicates they were done for the ith microwave passband. If the correlation length of the fluctuations in the plasma (distance over which they are correlated with themselves) is of the order of the crossing length of the two sightlines [$\approx 2w(z)$], and both are much less than the scale length for the turbulence to change amplitude, then a plot of C_{12i} vs the central frequency ω_i will plot out the linewidth of the ECE emission in the crossing volume versus frequency. If this is done for many time points (for instance, time points separated by T, the averaging time used in calculating the correlation functions), then the movement of the line center versus time will plot out the fluctuations of the magnetic field at frequencies less than $1/T$. This is true only if the estimated uncertainty in the line center is less than the magnetic field fluctuation. Thus a crucial part of the calculation is the estimate of the position of the line center and its uncertainty, by fitting some theoretical or heuristic function to the data. The actual expected line shape will be discussed further below, but it might well be Gaussian. If a Gaussian is fitted to the correlation-function-versus-frequency data, then it will be necessary to find three parameters—the amplitude, the center frequency, and the standard deviation of the Gaussian—and then estimate the uncertainty in the line center.

B. Correlation

The correlation functions are defined by[26]

$$R_{lk} = \lim_{T\to\infty}\frac{1}{T}\int_0^T I_l(t)I_k(t)dt = C_{lk} \quad (\mu_l=\mu_k=0), \tag{13}$$

where R_{lk} is precisely the cross-correlation function, and C_{lk} is more precisely the cross-covariance function. For $\mu_l=\mu_k=0$, R_{lk} and C_{lk} are identical. It will be assumed for simplicity (the average can always be subtracted out) that this is the case, and, as before, C_{lk} will be identified as the cross-correlation function. The quantities μ_l and μ_k are the average values of I_l and I_k. For $l=k$, C_{ll} is the autocorrelation function. The cross-correlation coefficient is defined by

$$\rho_{lk} = C_{lk}/(C_{ll}C_{kk})^{1/2}. \tag{14}$$

The cross-correlation coefficient takes on values from $+1$ to -1, and measures the degree of linear correlation of the functions I_l and I_k. If they are perfectly correlated or anticorrelated, then $\rho_{lk}=\pm 1$. For linearly related functions, less than 100% correlation implies the presence of noise.

The above definitions also assume that the data are ergodic, that is, the data are stationary in time, and time averages are equivalent to ensemble averages. While this is not strictly true, for the short time scales over which we plan to average (10 μs–1 ms), it is close enough. For actual calculation of the cross-correlation functions, we are left with the choice of using the definition above or calculating them from the Fourier transforms of the data.[26] It is currently expected to be faster to calculate them from the Fourier transforms. In estimating the correlation functions for finite periods T, there are some subtleties in the algorithms of which the analyst should be wary (see Bendat and Piersol[26] for a discussion).

C. Expected line shape

The expected line shape of the cross-correlation function versus frequency becomes rather difficult to discuss, since it depends on the natural spatial linewidth (l_{ns}) of the ECE (the relativistic broadening for perpendicular viewing), the correlation length (l_c) and shape of the correlation function in the plasma, the crossing length of the two sightlines in the plasma ($2w_0$), and the fluctuation wavelength(s). In the particular case being investigated it is expected that l_{ns}, l_c, and $2w_0$ will of be the same order. The natural linewidth (full width at half-maximum) will be given by[27]

$$\delta\omega/s\omega_b = c_s(v_{te}/c)^2, \tag{15}$$

where v_{te} is the electron thermal velocity [but is defined as $v_{te}=(T/m)^{1/2}$ rather than the more standard $(2T/m)^{1/2}$]. Here s is the harmonic number, and c_s is a constant which changes with harmonic number. For $s=3$, $c_s=4.8$.

It is expected that the density correlation function will have a Gaussian profile[24] with $l_c\approx 1$ cm, and the sightline crossing length is expected also to be the order of a centimeter. The natural linewidth can be considered as an equivalent spatial linewidth

$$l_{ns} = (B/\nabla B)c_s(v_{te}/c)^2. \tag{16}$$

For $T_e=750$ eV and for TEXT, $l_{ns}=7$ mm. The expected correlation linewidth is thus of the order of 7×10^{-3} of the line center ($\delta R/R_0=7\times10^{-3}$), and it is reasonably probable that it will have close to a Gaussian shape. It can be inferred from the above that there is some motivation to try

for smaller waists on the antenna patterns, which argues for higher harmonics. However, absolute signal levels could then be a problem. This is still being studied.

The actual correlation length in the plasma can be measured by calculating ρ_{12} at every ω_i and plotting it. If ρ_{12} is small at all frequencies in the crossing volume, then it can be inferred that the correlation length is very short compared to the crossing length. If ρ_{12} is comparatively large (say >0.5) for frequencies extending beyond the natural frequencies in the crossing volume, then the correlation length is longer than the crossing length and can be computed as $l_c = (\nabla B/B)(\delta\omega/\omega)$, where $\delta\omega$ is the frequency width of ρ_{12}. The optimum situation for measuring the magnetic field fluctuations would be to have the correlation length the same as the natural linewidth. It may be possible to force this situation by adjusting the correlation period T.

D. Fitting the data

Both linear and nonlinear FORTRAN routines are readily available (see, for instance, the book by Bevington[28]) for least-squares fitting of the data. If Gaussian line shapes turn out to be appropriate, then a fast linearized iterative nonlinear fitting routine developed for ISX-B is available to analyze the data. It would be otherwise preferable not to have to do nonlinear analysis, because of the possible slow performance of these routines.

E. Uncertainties

The crux of the data analysis is the estimation of the uncertainty in the calculation of the line center. There are several possible sources of uncertainty, but the bottom line is noise in the data (uncorrelated signal), and error due to using a finite T (time) in the correlation calculation or Fourier transform. The estimated error from both sources in the cross-correlation functions is[26]

$$\epsilon_C^2 \equiv \sigma^2/C_{ik}^2 = (1+\rho_{ik}^{-2})/N, \tag{17}$$

where N is the number of data points averaged over in calculating C_{ik} and ρ_{ik}, and σ is the standard deviation of C_{ik}.

Translating this into an uncertainty in the line center is not trivial, but it can be numerically estimated[28] at the least. For instance if $N=50$ and $\rho_{12}=0.50$, then $\epsilon_C=0.32$. To turn this into an estimate of the uncertainty in ω, it is necessary to know how much ω would have to vary to give this much uncertainty in C_{12}. For instance, one could assume a Gaussian line shape with some width $\Delta\omega$ and ask what frequency change $\delta\omega$ would be necessary to give the same change in C_{12}. Then the expected uncertainty in the line center (assume K frequency channels) would be

$$(\delta\omega)^2 = \sum_{i=1}^{K} (\delta\omega_i)^2 \Big/ K^2. \tag{18}$$

The exact value of course would depend on the details of the data, which is why we are doing our best to perform a good simulation of the experiment.

ACKNOWLEDGMENTS

Discussions with Dr. Peter Politzer contributed materially to the ideas in this paper, and it is a pleasure to acknowledge his contribution. Work leading to this paper was supported by the U.S. Department of Energy, Office of Fusion Energy, under contract No. DE-FG05-87ER53253, and by the Georgia Institute of Technology.

[a]The abstract for this paper appears in the *Proceedings of the 7th Topical Conference on High Temperature Plasma Diagnostics*, Rev. Sci. Instrum. **59**, 1644 (1988).
[1]L. A. Artsimovich, Nucl. Fusion **12**, 215 (1972).
[2]H. P. Furth, Nucl. Fusion **15**, 487 (1985).
[3]P. C. Liewer, Nucl. Fusion **25**, 543 (1985).
[4]T. H. Dupree, Phys. Fluids **10**, 1049 (1967).
[5]T. H. Dupree and D. J. Tetreault, Phys. Fluids **21**, 425 (1977).
[6]J. D. Callen, Phys. Rev. Lett. **39**, 1540 (1977).
[7]K. Molvig, J. E. Rice, and M. S. Tekula, Phys. Rev. Lett. **41**, 1240 (1978).
[8]C. E. Thomas, Jr., in Proceedings of the EC6 Joint Workshop on ECE and ECRH, Sept. 16-17, 1987, Oxford, United Kingdom (to be published).
[9]J. C. Wiltse *et al.*, Advances in Millimeter Wave Applications, 1–4 February 1988, Georgia Tech Education Extension Services, course notes.
[10]H. Kogelnik and T. Li, Appl. Opt. **5**, 1550 (1966).
[11]G. L. Bell, R. F. Gandy, J. B. Wilgen, and D. A. Rasmussen, Auburn University Physics Report No. PR21, Technical Report No. MMESI-19x-5596V-2, October 1987.
[12]A. Yariv, *Quantum Electronics* (Wiley, New York, 1967).
[13]K. Kato and I. H. Hutchinson, Rev. Sci. Instrum. **57**, 1959 (1986).
[14]K. Kato, Ph.D. thesis, Plasma Fusion Center, Massachusetts Institute of Technology, 1986 (Report No. PFC/RR-86-20).
[15]A. E. Costley, R. J. Hastie, and J. W. M. Chamberlain, Phys. Rev. Lett. **33**, 758 (1974).
[16]D. A. Boyd, F. J. Stauffer, and A. W. Trivelpiece, Phys. Rev. Lett. **37**, 98 (1976).
[17]G. D. Tait, F. J. Stauffer, and D. A. Boyd, Phys. Fluids **24**, 719 (1981).
[18]G. Taylor, P. C. Efthimion, M. P. McCarthy, E. Fredd, and R. C. Cutler, Rev. Sci. Instrum. **57**, 1974 (1986).
[19]C. M. Celata and D. A. Boyd, Nucl. Fusion **17**, 735 (1977).
[20]D. B. Batchelor and R. C. Goldfinger, Oak Ridge National Laboratory Report No. ORNL/TM-6844, 1982.
[21]D. J. Rose and M. Clark, Jr., *Plasmas and Controlled Fusion* (MIT, Cambridge, MA, 1965), p. 246.
[22]M. A. Heald and C. B. Wharton, *Plasma Diagnostics with Microwaves* (Wiley, New York, 1965), p. 275.
[23]G. Bekefi, *Radiation Processes in Plasmas* (Wiley, New York, 1966), p. 52.
[24]C. M. Surko and R. E. Slusher, Phys. Fluids **23**, 2429 (1980).
[25]A. Cavallo and R. Cano, Plasma Phys. **23**, 65 (1981).
[26]J. S. Bendat and A. G. Piersol, *Random Data: Analysis and Measurement Procedures*, 2nd ed. (Wiley–Interscience, New York, 1986).
[27]M. Bornatici, R. Cano, O. DeBarbieri, and F. Engelman, Nucl. Fusion **23**, 1153 (1983).
[28]P. R. Bevington, *Data Reduction and Error Analysis for the Physical Sciences* (McGraw-Hill, New York, 1969).